Data Sheet (Cat.No.T1020)

TargetMol

Doxorubicin hydrochloride

Chemical Properties

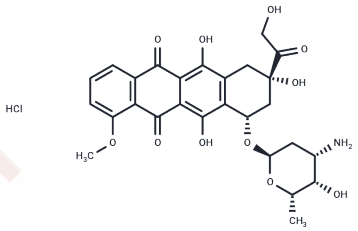

CAS No. : 25316-40-9

Formula: C27H29NO11·HCl

Molecular Weight: 579.99

Appearance: no data available

Storage: Powder: -20°C for 3 years | In solvent: -80°C for 1 year

Biological Description

Description	Doxorubicin hydrochloride (Adriamycin) belongs to the anthracycline class of antibiotics and is an inhibitor of human DNA topoisomerase I/II (IC50=0.8/2.67 μM). Doxorubicin hydrochloride exhibits cytotoxicity and antitumor activity. Doxorubicin hydrochloride reduces the phosphorylation of AMPK and its downstream target protein acetyl coenzyme A carboxylase, and induces apoptosis and autophagy.
Targets(IC50)	Apoptosis,Mitophagy,HIV Protease,Antibacterial,Antibiotic,AMPK,Autophagy,ADC Cytotoxin,HBV,Topoisomerase
In vitro	**METHODS**: Human breast cancer cells MCF10A, BT474, MCF-7 and T47D were treated with Doxorubicin hydrochloride (0.1-10 μM) for 48 h, and cell growth inhibition was detected by MTT. **RESULTS**: Doxorubicin hydrochloride dose-dependently inhibited the growth of MCF10A, BT474, MCF-7 and T47D cells with IC50s of 2.51 μM, 1.14 μM, 0.69 μM and 8.53 μM, respectively. [1] **METHODS**: Bovine aortic endothelial cells BAECs and human ovarian teratoma cells PA-1 were treated with Doxorubicin (0.5 μM) for 1-16 h. Apoptosis was detected by Flow Cytometry, and caspase-3 activity was detected by caspase-3 assay kit. **RESULTS**: Doxorubicin induced apoptosis and caspase-3 activation in BAECs and PA-1 cells in a time-dependent manner. [2] **METHODS**: Canine breast cancer cells CIPp were treated with Doxorubicin (EC50(20h) =12.08 μM) for 3-48 h. The expression of target genes was detected by qRT-PCR. **RESULTS**: Doxorubicin induced up-regulation of the mRNA expression levels of multidrug resistance (MDR)-related genes P-gp and BCRP. [3]
In vivo	**METHODS**: To detect antitumor activity in vivo, Doxorubicin hydrochloride (1 mg/kg/4 days) and lovastatin (5 mg/kg/day) were intraperitoneally injected into B6D2F1 mice bearing murine melanoma tumor B16F10 for two weeks. **RESULTS**: The combination of Doxorubicin hydrochloride and lovastatin showed a significant increase in sensitivity compared to either drug alone. lovastatin enhanced the antitumor activity of Doxorubicin hydrochloride. [4] **METHODS**: To investigate the acute and long-term cognitive deficits of Doxorubicin in cancer patients, a single dose of Doxorubicin hydrochloride (25 mg/kg) was administered intraperitoneally to B6C3F1J mice. **RESULTS**: Systemic treatment with Doxorubicin hydrochloride altered glutamatergic neurotransmission in the nucleus of key cells associated with cognitive function within 24 h. There were no lasting effects on spatial learning and memory. [5]

Cell Research	To analyze the effect of Bcl-2 expression on the viability of HUVECs treated with Dox, cells were co-transfected with 200 ng of the pEGFP-spectrin expression plasmid together with 200 ng of either pCDNA3-hBcl-2 or the control pCMVβ-galactosidase expression vector (33). The pGL3 Basic vector (2.1 μg) was added as a DNA carrier in a total volume of 0.140 ml, and transfection was performed by the calcium phosphate procedure in 35-mm tissue culture dishes. After treatment, the cells were washed with PBS, fixed with 3.7% formaldehyde for 15 min, and washed for a further 10 min with 50 mM NH4Cl blocking solution in PBS. Cells were then washed with PBS, permeabilized with a 0.1% Triton X-100 for 10 min, washed again with PBS, and stained with 1 μg/ml 4′,6-diamidino-2-phenyl-indole solution for 2 min. The cells were examined under a fluorescence microscope, and GFP-positive cells were scored after counting a minimum of 1000 total cells for each condition. The efficiency of transfection in Bcl-2- and β-galactosidase-expressing cells, determined in aliquots of transfected cells just before the addition of Dox, was similar (10–12%) [1].
Animal Research	Athymic male nude mice (3-4 weeks old) are used. PC3 cells (4×106) are injected subcutaneously into the flanks of mice. Animals bearing tumors are randomly assigned to treatment groups (five or six mice per group) and treatment initiated when xenografts reached volumes of about 100 mm3. Tumors are measured using digital calipers and volume calculated using the formula: Volume=Width2×Length×0.52, where width represents the shorter dimension of the tumor. Treatments are administered as indicated using vehicle (PBS containing 0.1% BSA), Doxorubicin (2-8 mg/kg), Apo2L/TRAIL (500 μg/animal), or a combination of 4 mg/kg Doxorubicin followed by 500 μg Apo2L/TRAIL. Doxorubicin is administered systemically whereas Apo2L/TRAIL is given either intratumorally or systemically. All treatments are given once. Mice are monitored daily for signs of adverse effects (listlessness and scruffy appearance). Treatments seemed to be well tolerated. The mean±SEM is calculated for each data point. Differences between treatment groups are analyzed by the student t-test. Differences are considered significant when P<0.05 [3]. Altogether, 29 male Wistar rats (weight 306 ± 18.6 g) were used in the study. Animals were divided into three groups: control (group C; n = 10; 306.4 ± 17.2 g), animals treated with DOX (group DOX; n = 10; 305.0 ± 24.9 g) and animals treated with L-DOX (group L-DOX; n = 9; 306.7 ± 15.0 g). Vehiculum (aqua pro injection), DOX and L-DOX were applied to group C, DOX and L-DOX, respectively, by single intraperitoneal injection; concentration of both DOX and L-DOX was 5 mg/kg, similar to the concentrations used in human treatment protocols. All animals were sacrificed 24 h after drug application. Thoracotomy was performed, hearts were excised and samples were obtained separately from the free wall of the left atrium (LA), left ventricle (LV), right atrium (RA) and right ventricle (RV).Samples were placed into RNA later preservation solution and stored at -80 C until further analysis [4].

Solubility Information

Solubility	DMSO: 55 mg/mL (94.83 mM),Sonication is recommended. H2O: 50 mg/mL (86.2 mM),Sonication is recommended. (< 1 mg/ml refers to the product slightly soluble or insoluble)

Preparing Stock Solutions

	1mg	5mg	10mg
1 mM	1.7242 mL	8.6208 mL	17.2417 mL
5 mM	0.3448 mL	1.7242 mL	3.4483 mL
10 mM	0.1724 mL	0.8621 mL	1.7242 mL
50 mM	0.0345 mL	0.1724 mL	0.3448 mL

Please select the appropriate solvent to prepare the stock solution, according to the solubility of the product in different solvents. Please use it as soon as possible.

Reference

Wen SH, et al. Sulbactam-enhanced cytotoxicity of doxorubicin in breast cancer cells. Cancer Cell Int. 2018 Sep 4; 18:128.
Wang B, Jin Y, Liu J, et al.EP1 activation inhibits doxorubicin-cardiomyocyte ferroptosis via Nrf2.Redox Biology. 2023: 102825.
Zhang L, Feng M, Wang X, et al. Peptide Szeto-Schiller 31 ameliorates doxorubicin-induced cardiotoxicity by inhibiting the activation of the p38 MAPK signaling pathway. International Journal of Molecular Medicine. 2021, 47 (4): 1-11
Lu J, Li J, Hu Y, et al. Chrysophanol protects against doxorubicin-induced cardiotoxicity by suppressing cellular PARylation[J]. Acta Pharmaceutica Sinica B. 2018 Nov
Lu J, Li J, Hu Y, et al. Chrysophanol protects against doxorubicin-induced cardiotoxicity by suppressing cellular PARylation. Acta Pharmaceutica Sinica B. 2018 Nov
Zuo Z, Shen J X, Pan Y, et al. Weighted gene correlation network analysis (WGCNA) detected loss of MAGI2 promotes chronic kidney disease (CKD) by podocyte damage. Cellular Physiology and Biochemistry. 2018;51(1): 244-261
Wang Y, Wu Y, Chen Y, et al. Nanoliter Centrifugal Liquid Dispenser Coupled with Superhydrophobic Microwell Array Chips for High-Throughput Cell Assays. Micromachines. 2018 Jun 6;9(6)
Yıldızhan K, Huyut Z, Altındağ F. Involvement of TRPM2 Channel on Doxorubicin-Induced Experimental Cardiotoxicity Model: Protective Role of Selenium. Biological Trace Element Research. 2022: 1-12.
Tang K, Zhang X, Guo Y. Identification of the dietary supplement capsaicin as an inhibitor of Lassa virus entry. Acta Pharmaceutica Sinica B. 2020
Liang C, Yu X, Xiong N, et al. Pictilisib Enhances the Antitumor Effect of Doxorubicin and Prevents Tumor-Mediated Bone Destruction by Blockade of PI3K/AKT Pathway. Frontiers in oncology. 2020, 10.
Yıldızhan K, Huyut Z, Altındağ F Involvement of TRPM2 Channel on Doxorubicin-Induced Experimental Cardiotoxicity Model: Protective Role of Selenium. Biological Trace Element Research. 2022: 1-12
Zhong Y, Li M, Zhang X, et al. Dissecting Chemical Composition and Cardioprotective Effects of Fuzhengkangfu Decoction against Doxorubicin-Induced Cardiotoxicity by LC–MS and Bioinformatics Approaches. ACS Omega. 2020
Gaweł, Agata M., et al. Analysis of the Role of FRMD5 in the Biology of Papillary Thyroid Carcinoma. International Journal of Molecular Sciences. 22.13 (2021): 6726.
Li J, Sun Y, Zhao X, et al.Radiation induces IRAK1 expression to promote radioresistance by suppressing autophagic cell death via decreasing the ubiquitination of PRDX1 in glioma cells.Cell Death & Disease.2023, 14(4): 1-16.
Wang S, et al. Doxorubicin induces apoptosis in normal and tumor cells via distinctly different mechanisms. intermediacy of H(2)O(2)- and p53-dependent pathways. J Biol Chem. 2004 Jun 11;279(24):25535-43.
Xu H, You H, Gong J, et al.Discovery of Zidovudine as a cardiomyocyte protectant for doxorubicin-induced toxicity through high-throughput phenotypic drug screening.Fundamental Research.2023
Hou Z, Ren Y, Zhang X, et al.EP300-ZNF384 transactivates IL3RA to promote the progression of B-cell acute lymphoblastic leukemia.Cell Communication and Signaling.2024, 22(1): 211.
Dong C, Meng X, Zhang T, et al.Single-cell EpiChem jointly measures drug–chromatin binding and multimodal epigenome.Nature Methods.2024: 1-10.
Li Y, Wu W, Song Y, et al.β-Caryophyllene Confers Cardioprotection by Scavenging Radicals and Blocking Ferroptosis.Journal of Agricultural and Food Chemistry.2024
Ma G, Gao A, Chen J, et al.Modeling high-risk Wilms tumors enables the discovery of therapeutic vulnerability.Cell Reports Medicine.2024
Lu Y, Fang Y, Wang S, et al.Cepharanthine sensitizes gastric cancer cells to chemotherapy by targeting TRIB3-FOXO3-FOXM1 axis to inhibit autophagy.Phytomedicine.2024: 156161.
Ge W, Zhang X, Lin J, et al.Rnd3 protects against doxorubicin-induced cardiotoxicity through inhibition of PANoptosis in a Rock1/Drp1/mitochondrial fission-dependent manner.Cell Death & Disease.2025, 16(1): 1-16.
Yue Y, Li H, Wang X, et al.Intelligent Responsive Nanoparticles with Multilevel Triggered Drug Penetration for Tumor Photochemotherapy.ACS Applied Materials & Interfaces.2023
Levi M, et al. Doxorubicin treatment modulates chemoresistance and affects the cell cycle in two canine mammary tumour cell lines. BMC Vet Res. 2021 Jan 18;17(1):30.

Feleszko W, et al. Lovastatin potentiates antitumor activity of doxorubicin in murine melanoma via an apoptosis-dependent mechanism. Int J Cancer. 2002 Jul 1;100(1):111-8.
Rizwan A, Gulfam M, Jo S H, et al.Gelatin-based NIR and reduction-responsive injectable hydrogels cross-linked through IEDDA click chemistry for drug delivery application.European Polymer Journal.2023: 112019.
Bi X, Zhang M, Zhou J, et al.Phosphorylated Hsp27 promotes adriamycin resistance in breast cancer cells through regulating dual phosphorylation of c-Myc.Cellular Signalling.2023: 110913.
Thomas TC, et al. Acute treatment with doxorubicin affects glutamate neurotransmission in the mouse frontal cortex and hippocampus. Brain Res. 2017 Oct 1;1672:10-17.
Zhang L, Feng M, Wang X, et al. Peptide Szeto-Schiller 31 ameliorates doxorubicin-induced cardiotoxicity by inhibiting the activation of the p38 MAPK signaling pathway[J]. International Journal of Molecular Medicine. 2021, 47(4): 1-11
Wang H, Shi J, Tang B, et al.Forecast and verification of the active compounds and latent targets of Guyuan decoction in treating frequently relapsing nephrotic syndrome based on network pharmacology.Renal Failure. 2023, 45(1): 2184654.
Hu Y, Liu J, Lu J, et al. sFRP1 protects H9c2 cardiac myoblasts from doxorubicin-induced apoptosis by inhibiting the Wnt/PCP-JNK pathway[J]. Acta Pharmacologica Sinica. 2020: 1-8.
Hu Y, Liu J, Lu J, et al. sFRP1 protects H9c2 cardiac myoblasts from doxorubicin-induced apoptosis by inhibiting the Wnt/PCP-JNK pathway. Acta Pharmacologica Sinica. 2020: 1-8.
Wang H, Wang Q, Cai G, et al. Nuclear TIGAR mediates an epigenetic and metabolic autoregulatory loop via NRF2 in cancer therapeutic resistance. Acta Pharmaceutica Sinica B. 2021
Zuo Z, Shen J X, Pan Y, et al. Weighted gene correlation network analysis (WGCNA) detected loss of MAGI2 promotes chronic kidney disease (CKD) by podocyte damage[J]. Cellular Physiology and Biochemistry. 2018;51(1): 244-261.
Tang K, Zhang X, Guo Y. Identification of the dietary supplement capsaicin as an inhibitor of Lassa virus entry[J]. Acta Pharmaceutica Sinica B. 2020.
Lü Z, Li X, Li K, et al. Nitazoxanide and related thiazolides induce cell death in cancer cells by targeting the 20S proteasome with novel binding modes. Biochemical Pharmacology. 2022: 114913.